# Evolution of gaseous disk viscosity driven by supernova explosion in star-forming galaxies at high redshift

Jian-Min Wang<sup>1,2</sup>, Chang-Shuo Yan<sup>1,3</sup>, Yan-Rong Li<sup>1,3</sup>, Yan-Mei Chen<sup>1,3</sup>, Fei Xiang<sup>1</sup>, Chen Hu<sup>1</sup>, Jun-Qiang Ge<sup>1,3</sup>, and Shu Zhang<sup>1</sup>

#### ABSTRACT

Motivated by Genzel et al.'s observations of high-redshift star-forming galaxies, containing clumpy and turbulent rings or disks, we build a set of equations describing the dynamical evolution of gaseous disks with inclusion of star formation and its feedback. Transport of angular momentum is due to "turbulent" viscosity induced by supernova explosions in the star formation region. Analytical solutions of the equations are found for the initial cases of a gaseous ring and the integrated form for a gaseous disk, respectively. For a ring with enough low viscosity, it evolves in a slow processes of gaseous diffusion and star formation near the initial radius. For a high viscosity, the ring rapidly diffuses in the early phase. The diffusion drives the ring into a region with a low viscosity and start the second phase undergoing pile-up of gas at a radius following the decreased viscosity torque. The third is a sharply deceasing phase because of star formation consumption of gas and efficient transportation of gas inward forming a stellar disk. We apply the model to two  $z \sim 2$  galaxies BX 482 and BzK 6004, and find that they are undergoing a decline in their star formation activity.

Subject headings: galaxies: evolution – galaxies: high-redshift

#### 1. Introduction

Exciting progress has been made in observing assembly of gas and star formation in galaxies from low to high redshifts. Optically/UV-selected star-forming galaxies at  $z\sim$ 

<sup>&</sup>lt;sup>1</sup>Key Laboratory for Particle Astrophysics, Institute of High Energy Physics, Chinese Academy of Sciences, 19B Yuquan Road, Beijing 100049, China

<sup>&</sup>lt;sup>2</sup>Theoretical Physics Center for Science Facilities, Chinese Academy of Sciences, China

<sup>&</sup>lt;sup>3</sup>Graduate University of Chinese Academy of Sciences, 19A Yuquan Road, Beijing 100049, China

0.5 - 2.5 exhibit a fairly tight relationship between stellar mass and star formation rate, which is strongly suggestive of star formation happening with a high duty cycle (Noeske et al. 2007; Elbaz et al. 2007; Daddi et al. 2007). This may relate with random accretion onto supermassive black holes (SMBHs) triggered through minor mergers located at galactic centers (Wang et al 2009), showing episodic activities of the SMBHs (Wang et al. 2006, 2008). Major mergers are undoubtedly taking place in very luminous submillimeter galaxies at  $z \sim 1 - 3$  (Tacconi et al. 2006; 2008), but only a small fraction of this sample ( $\sim 1/3$ ) is undergoing obvious major mergers from the images of the sample (Föster Schreiber et al. 2006; Genzel et al. 2006; Wright 2007; Law et al. 2007). Detail studies of Spectroscopic Imaging survey in the Near-infrared with SINFONI (SINS) of high-redshift galaxies show that about 1/3 of the samples are rotation-dominated turbulent star-forming rings/disks; another one-third are compact and velocity dispersion-dominated objects and the remains are clear interacting/merging systems (Genzel et al. 2008; Föster Schreiber et al. 2009). These dynamical evidences show that rapid and continuous gas accretion via "cold flows" and/or minor mergers are playing an important role in driving star formation and assembly of star-forming galaxies at z > 1 (Genzel et al. 2008). Interestingly, recent numerical simulations produce results agreeing with the observations (Bower et al. 2006; Kitzbichler & White 2007; Naab et al. 2007; Guo & White 2008; Davé 2008; Brooks et al. 2009; Dekel et al. 2009). Minor mergers as a supply of gas may trigger star formation and subsequently ignite the SMBHs. The role of supernova explosions (SNexp) in driving interstellar turbulence and the existence of a supernova rate-velocity dispersion relation has been highlighted using numerical simulations (e.g., Wada & Norman 2002; Dib et al. 2006), and observationally by the spatial correlations of the inclinations of molecular clouds with respect to the Galactic disk attributed to the effects of SNexp (Dib et al. 2009; see an extensive review of Mac Low & Klessen 2004), and by the existence of a starburst-AGN connection (Chen et al. 2009). SNexp is potentially playing a role in the dynamics in star-forming galaxies.

Distributions of density and angular momentum of a gaseous disk are generally controlled by the viscosity, if driven by viscosity of turbulence excited by SNexp, stellar distribution will be determined by this feedback process (Lin & Pringle 1987). Steady analytical solution of circumnuclear disk of the Galaxy with injection of SNexp energy has been obtained by Vollmer & Beckert (2003), coevolution of SMBHs and their hosts could be driven by SNexp-excited turbulence (Kawakatu & Wada 2008) as well as in the starburst–AGN connection in light of strong correlation between the Eddington ratios and specific star formation rates (Chen et al. 2009). Figure 1 shows a clear trend of concentration of galaxies with star formation rate densities in the SINS sample given by Genzel et al. (2008), strengthening the interplay and regulation between SN explosions, cold gas accretion, and minor mergers.

In this Letter, we consider the secular evolution of gaseous disk, which could be formed

during minor mergers, by including feedback from SNexp in star formation or burst regions characterized by the H $\alpha$  ring in the SINS sample. We find the analytical solutions, which show two kinds of properties: 1) piled-up gas and 2) fast diffusion depending on the initial conditions of gas density. We apply the models to high-redshift galaxies.

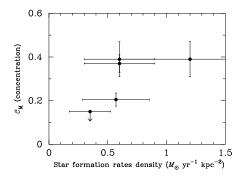


Fig. 1.— Mass concentration of galaxies defined by a ratio of dynamical mass within 0".4-1".2,  $C_{\rm M} = M_{\rm dyn} (\leq 0".4)/M_{\rm dyn} (\leq 1".2)$ , correlates with star formation rates for the SINS sample given in Table 2 in Genzel et al. (2008). This correlation strengthens the role of SNexp.

#### 2. Dynamical equations

Considering the mass dropout of gaseous disk due to ongoing star formation, the mass conservation equation reads

$$R\frac{\partial \Sigma}{\partial t} + \frac{\partial}{\partial R} (RV_{\rm R}\Sigma) + R\dot{\Sigma}_{\star} = 0, \tag{1}$$

where  $V_{\rm R}$  is the radial velocity of the gas,  $\Sigma$  is the surface density of gas, and  $\Sigma_{\star}$  is the surface density of star formation rates. We neglect mass injection of stellar winds back to the gaseous disk or escapes of winds from galaxies. Star formation process removes some angular momentum of gas, thus the conservation equation of angular momentum is given by

$$R\frac{\partial}{\partial t} \left( \Sigma R^2 \Omega \right) + \frac{\partial}{\partial R} \left( R V_R \Sigma R^2 \Omega \right) - \frac{1}{2\pi} \frac{\partial \mathcal{G}}{\partial R} + R^3 \Omega \dot{\Sigma}_{\star} = 0, \tag{2}$$

where  $\mathcal{G} = 2\pi R^3 \nu \Sigma \left( d\Omega/dR \right)$  is the viscosity torque,  $\nu$  is kinematic viscosity, and  $\Omega$  is the angular velocity. Combining eqs. (1) and (2), we have

$$\frac{\partial \Sigma}{\partial t} = -\frac{1}{2\pi R} \frac{\partial}{\partial R} \left\{ \left[ \frac{d \left( R^2 \Omega \right)}{dR} \right]^{-1} \frac{\partial \mathcal{G}}{\partial R} \right\} - \dot{\Sigma}_{\star}. \tag{3}$$

In this Letter, we explore the role of viscosity driven by SNexp in the secular evolution of gaseous disk. Similar to Kawakatu & Wada (2008), we assume that the vertical structure is

supported by turbulence pressure

$$\frac{P_{\text{tur}}}{H} = \rho_{\text{g}} \left( \frac{GM_{\bullet}H}{R^3} + \pi G\Sigma \right) \approx \rho_{\text{g}} \frac{\sigma^2}{R}, \tag{4}$$

where  $M_{\bullet}$  is the black hole mass, G is the gravity constant,  $\Omega = \sqrt{2}\sigma/R$  and  $\pi G\Sigma = \sigma^2/R$  are used (eq. 1 in Thompson et al. 2005),  $P_{\rm tur} = \rho_{\rm g}V_{\rm tur}^2$  is the turbulence pressure,  $\sigma$  is the dispersion velocity of galaxies determined by the total potential of gas, stars, and dark matter halo, and H is the half-thickness of the disk. The validity of solutions presented here is limited by the potential used in eq. (4), namely,  $GM_{\bullet}H/R^3 \lesssim \sigma^2/R$ , we thus have,  $R \gtrsim GM_{\bullet}(H/R)/\sigma^2 \sim 10~M_8\sigma_{200}^2(H/R)$ pc, where  $M_8 = M_{\bullet}/10^8M_{\odot}$  and  $\sigma_{200} = \sigma/200~{\rm km~s^{-1}}$ . The energy equation of turbulence excited by SNexp is given by Wada & Norman (2002)

$$\frac{\rho_{\rm g} V_{\rm tur}^2}{t_{\rm dis}} = \frac{\rho_{\rm g} V_{\rm tur}^3}{H} = \xi \dot{S}_{\star} E_{\rm SN},\tag{5}$$

where  $t_{\rm dis} = H/V_{\rm tur}$  is the timescale of the turbulence,  $\xi$  is the efficiency converting kinetic energy of SNexp into turbulence,  $\dot{S}_{\star}$  is the SNexp rate, and  $E_{\rm SN}$  is the SNexp energy. SNexp rate strongly depends on the initial mass functions, but we absorb its uncertainties into the parameter  $\xi$  and simply let  $\dot{S}_{\star}$  be the star formation rate.

The viscosity law  $\nu = \alpha V_{\rm tur} H$  is assumed commonly, where  $\alpha$  is the viscosity parameter (Shakura & Sunyaev 1973). The Kennicutt–Schmidt's law displays  $\dot{\Sigma}_{\star} \propto \Sigma^{1.4}$ , however, there are growing evidence for a linear relation for denser environment in star-forming galaxies from numerical simulations (Dobbs & Pringle 2009; Krumholz et al. 2009). We use  $\dot{\Sigma}_{\star} = c_{\star} \Sigma$  for star-forming galaxies at high-redshift, where  $c_{\star}$  is a constant. We thus have the energy equation  $V_{\rm tur}^3 = \xi c_{\star} H E_{\rm SN}$ , where  $c_{\star}$  is the efficiency converting gas into stars. With the help of equations (4) and (5), we have

$$\nu(R) = \zeta R^4 = 0.128 \,\zeta_{0.128} R_1^4 \,\text{kpc}^2 \,\text{Gyr}^{-1},\tag{6}$$

where  $\zeta = \alpha \left(\xi c_{\star} E_{\rm SN}\right)^3/\sigma^8 = 0.128\alpha_{0.1} \left(\xi_{-3} c_{-8} E_{51}\right)^3 \sigma_{200}^{-8} \ \text{kpc}^{-2} \text{Gyr}^{-1}$ ,  $R_1 = R/1 \ \text{kpc}$ ,  $\alpha_{0.1} = \alpha/0.1$ ,  $E_{51} = E_{\rm SN}/10^{51} \text{erg}$ ,  $\xi_{-3} = \xi/10^{-3} M_{\odot}^{-1}$ , and  $c_{-8} = c_*/3 \times 10^{-8} \ \text{yr}^{-1}$ . Here, the star formation efficiency is assumed to be a constant independent of the gas density and radius. Such strong dependence of viscosity on the radius means that transportation of angular momentum will be much more efficient at outer radii than at the inner.

The star surface density can be obtained from

$$\Sigma_*(R,t) = \int_0^t \dot{\Sigma}_* dt' = \int_0^t c_* \Sigma(R,t') dt'. \tag{7}$$

Vertical self-gravity may directly control the star formation as suggested by Thompson et al. (2005). We test self-gravity of the disk through Toomre parameter Q, defined by

 $Q = c_s \kappa_\Omega/\pi G\Sigma \propto \Sigma^{-1}$ , where  $\kappa_\Omega^2 = 4\Omega^2 + d\Omega^2/d \ln r$  is the epicyclic frequency,  $c_s = 1.0T_2^{1/2}$  km s<sup>-1</sup>is the sound speed, and  $T_2 = T/10^2$ K is the gas temperature (Kawakatu & Wada 2008). We should keep in mind that there are two different aspects from the classical gaseous disk investigated by Lynden-Bell & Pringle (1974): (1) radius-dependent viscosity driven by SNexp and (2) dropout of mass and angular momentum due to star formation on the disk. These drive some interesting properties of gaseous disks.

## 3. Solutions: evolutionary properties

#### 3.1. Gaseous ring

A realistic initial condition is a single gaseous ring, which can be formed via one minor merger (Hernquist & Mihos 1995). Equations (3-6) have analytical solutions for the case of a single ring. After some algebraic operations (e.g., Kato et al. 1998), we have the analytical solution for the case

$$\Sigma(r,\tau) = \frac{\Sigma_0}{2\pi^{\frac{1}{2}}} \frac{1}{r^4} \left(\frac{q_0}{\tau}\right)^{\frac{1}{2}} \left(1 - e^{-\frac{4q_0}{\tau r}}\right) e^{-\tau - \frac{q_0}{\tau} \left(\frac{1}{r} - 1\right)^2},\tag{8}$$

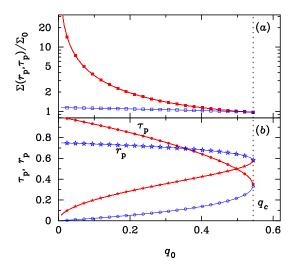


Fig. 2.— Properties of the surface density  $\Sigma(r,\tau)$  as to  $q_0$ . Here,  $r_{\rm p}$  and  $\tau_{\rm p}$  are solutions of  $\partial \Sigma/\partial r = 0$  and  $\partial \Sigma/\partial \tau = 0$ .  $\Sigma(r_{\rm p},\tau_{\rm p})$  is the peak or valley values at  $r_{\rm p}$  and  $\tau_{\rm p}$ . The red and blue points correspond to peak and valley of the density, respectively. The stars represent  $r_{\rm p}$ . When  $q_0 > q_{\rm c} = 0.544$ , there is no solution, namely, the density monotonously decreases with time and radius. All the hollow symbols are the valley of the envelope of the  $\Sigma$ -evolution track whereas the solid ones are its peak.

where  $\Sigma_0 = M_0/\pi R_0^2$ ,  $\tau = c_* t$ ,  $r = R/R_0$ , and  $M_0$  is the total mass of the initial ring at

a radius  $R_0$ , and the dimensionless parameter  $q_0$  is defined by

$$q_0 = \frac{c_*}{4\zeta R_0^2} = 0.584 \ \alpha_{0.1}^{-1} c_{-8}^{-2} R_{0,1}^{-2} (\xi_{-3} E_{51})^{-3} \sigma_{200}^8, \tag{9}$$

where  $R_{0,1} = R_0/10$  kpc.

Complicated evolutionary behaviors of the surface density are determined by  $q_0$  values as shown in Figure 2. For a given  $q_0 \leq q_c = 0.544$ , there are two sets of roots of  $\partial \Sigma(r,\tau)/\partial r = 0$  and  $\partial \Sigma(r,\tau)/\partial \tau = 0$ , corresponding to the peak and valley of the envelope

of  $\Sigma$ -evolution track at  $r_{\rm p}$  and  $\tau_{\rm p}$ . Otherwise there is no root of the two equations, namely there is no peak or valley of the envelope. Evolution of  $\Sigma(r,\tau)$  and  $\Sigma_*(r,\tau)$  can be found in Figure 3(a) and (b), respectively. We show three types of the solutions: (1)  $q_0 < q_c$ , (2)  $q_0 = q_c$ , and (3)  $q_0 > q_c$ . The  $q_0 > q_c$  solutions are quite simple and similar to the pure diffusion of a gaseous ring described in Lynden-Bell & Pringle (1974). The ring dramatically spreads over the space and forms stars. A stellar ring forms then as shown in Figure 3(b)  $q_0 = 2$  panel. For  $q_0 = q_c$  solution, there is a flat envelope without peak and valley, forming a very broader stellar ring as shown in the Figure 3(b)  $q_0 = 0.544$  panel.

The  $q_0 < q_c$  solutions have complicated behaviors as shown in Figure 3(a)  $q_0 = 0.1$  panel. Evolution of the gas ring can be divided into three phases. At early time, star formation is only important in the role of transportation of angular momentum, and the mass dropout can be neglected. Behaviors of the ring are very similar to the pure fluid ring. The gas rapidly diffuses inward mostly and outward a little bit carrying away the angular momentum. Though the star formation rates are very high, the total formed stars are not many since the duration of this phase is quite short. The second phase begins when mass dropout due to star formation becomes important. Decrease of the gas density is leading to decrease of star formation and weakening the viscosity torque of SNexp, resulting in accumulation of gas at the radius  $r_{\rm p}$ . The third phase starts when the viscosity torque is enhanced in light of the gas accumulation. This causes intensive star formation and exhausts gas, giving rise to an exponential decreases of gas density.

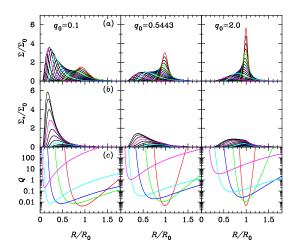


Fig. 3.— Evolution of gaseous ring and star surface densities for different parameter  $q_0$ . In top and middle panel, black lines show the evolution of gas and star disk from  $\tau_1 = 0.005$  to  $\tau_2 = 5$  with an interval  $\Delta \log \tau = 0.15$ . Red, green, blue, cyan, and pink lines in bottom panel represent the Toomre parameter Q at  $\tau = 0.005, 0.03, 0.2, 1, and 5$ , respectively, which correspond to the same meanings in panels (a) and (b). We set the surface density of gas is  $\Sigma_0 = 100 M_{\odot}$  pc<sup>-2</sup> to calculate the Toomre parameter for three different  $q_0$  values.

To understand such behaviors of solutions, we compare the timescales of star formation  $(t_* = 1/c_*)$  and gas advection  $(t_{\text{adv}} = R/V_R \approx R^2/\nu = 1/\zeta R^2)$ . According to the  $q_0$ -definition, it follows  $t_{\text{adv}}/t_* = 4q_0$ . When  $t_* \ll t_{\text{adv}}$  at  $R_0$  (roughly corresponding to  $q_0 \gg q_c$ ), most of the gas is converted into stars at  $R_0$  and only a little gas is conveyed inward. In contrast, in the  $t_* \gg t_{\text{adv}}$  case (namely,  $q_0 \ll q_c$ ) at initial radius  $R_0$ , star formation is so slow that most of the gas is advected inward. For a case with initial  $q_0 \ll q_c$ , most of gas is advected inward until  $t_{\text{adv}} > t_*$ . Pile-up of gas appears at  $r_p$  then and forms stars. The complicated behaviors of gas density are results as a consequence of competition between the two processes.

Figure 3(b) shows the surface density of stars for the corresponding gas density. For  $q_0 = 0.1$ , the gas rapidly diffuses inward and there is no significant pile-up of stars at the initial radius  $R_0$ . A stellar ring forms at roughly  $\sim 0.15R_0$  far away from its initial radius. The ring becomes broader with increases of  $q_0$ . When  $q_0 = q_c$ , there begins to be a tiny pile-up of stars at the initial radius. For a case with a large  $q_0$ , pile-up of stars happens very close to the initial radius and it becomes more conspicuous with  $q_0$ . The stellar rings become wider with  $q_0$ . Figure 3(c) displays evolution of the Toomre parameter Q, clearly showing Q < 1 in the star-forming region. Q-values are quite different in different regions. This strengthens the importance of self-gravity in the secular evolution of the gaseous disk. Since  $Q \propto \Sigma_{\rm gas}^{-1}$ , Q basically follows the evolution of  $\Sigma_{\rm gas}$ . A generic property of the Q-parameter is

that it increases with time since the gas is being converted into stars. This is totally different from the steady gaseous disk with star formation under the presumed condition of Q = 1 suggested by Thompson et al. (2005).

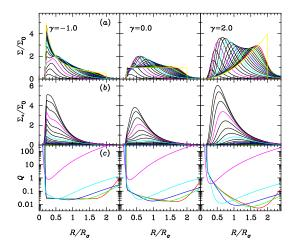


Fig. 4.— Evolution of gaseous disk and star surface densities for different initial disks. In the top and middle panel, black lines show the evolution of gas and star disk from  $\tau_1 = 0.005$  to  $\tau_2 = 5$  with an interval  $\Delta \log \tau = 0.15$ . Red, green, blue, cyan, and pink lines in bottom panel represent the Toomre parameter Q at  $\tau = 0.005, 0.03, 0.2, 1, and 5$ , respectively, which correspond to the same meanings with panels (a) and (b). We set the surface density of gas is  $\Sigma_0 = 100 M_{\odot}$  pc<sup>-2</sup> to calculate the Toomre parameter for three different  $\gamma$  values. The yellow lines in (a) are the initial surface densities.

We would like to point out that the feedback from SNexp will be enhanced, if we use the non-linear Kennicutt–Schmidt's law to calculate the star formation rate, leading to more efficient viscosity to transport angular momentum. However, the main features given by eq. (8) will remain. A detailed discussion on this nonlinear effects is beyond the scope of this Letter, but it would be interesting to solve the nonlinear equations to display the effects in future work. This model may apply to different kinds of galaxies.

### 3.2. Gaseous disk

Successive multiple minor mergers may provide an initial gas widely distributed in the major galaxies (Hernquist & Mihos 1995; Bournaud et al. 2007). For a simplicity, we assume an initial distribution with a power law of radius as  $\Sigma(R,0) = \Sigma_0 (R/R_\sigma)^\gamma$ , where  $R_\sigma = (c_*/4\zeta)^{1/2} = 7.65 \ c_{-8}^{1/2} \zeta_{0.128}^{-1/2}$  kpc,  $\Sigma_0$  is the surface density at  $R_\sigma$ , and  $\gamma$  is the index.

We integrate the Green's function over the radius range of the disk, and have

$$\Sigma(r_{\sigma}, \tau) = \int_{0}^{\infty} \frac{\Sigma(r_{0}, 0)}{(\pi \tau)^{\frac{1}{2}}} \frac{r_{0}^{2}}{r_{\sigma}^{4}} \left( 1 - e^{-\frac{2r_{0}^{-1}}{\tau r_{\sigma}}} \right) e^{-\tau - \frac{1}{\tau} \left( \frac{1}{r_{\sigma}} - \frac{1}{r_{0}} \right)^{2}} dr_{0}, \tag{10}$$

where  $r_{\sigma} = R/R_{\sigma}$  and  $r_0 = R_0/R_{\sigma}$ .

Figure 4 shows the evolution of gaseous disk. We calculate the cases of  $\gamma = -1.0, 0, and 2.0$  between  $R_1 = 0.2R_{\sigma}$  and  $R_2 = 2.0R_{\sigma}$ . For  $\gamma = -1.0$  disk, the most dense part of the disk is located in the radius with  $t_* < t_{\rm adv}$ , so the gas is converted to stars locally. In contrast, for  $\gamma = 2.0$  case gas is concentrated outside the region with  $t_* > t_{\rm adv}$ . The gas diffuses quite rapidly and transfers to the inner radius and forms stars, leaving a relatively broader stellar ring or disk. An initial homogeneous disk has a complex behaviors between the two cases above, inner part of the gas forms stars locally whereas outer part flows inward and then forms stars. The Toomre parameter shows strong variability with time, but holding Q < 1 in most star-forming region.

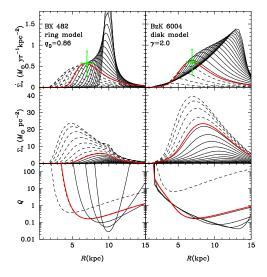


Fig. 5.— All the red thick lines are the current status of galaxy BX 482 and BzK 6004. Given  $\sigma = 210 \,\mathrm{km \ s^{-1}}$  from observations for the model parameters of BX 482, we relatively arbitrarily choose  $R_0 = 10 \,\mathrm{kpc}$ , then make out  $q_0 = 0.86$ . We have  $\Sigma_0 = 9.3 \,M_{\odot}$  pc<sup>-2</sup> from star formation rates. For Bzk 6004, we find that the initial parameters are  $\Sigma_0 = 69 \,M_{\odot}$  pc<sup>-2</sup>,  $R_1 = 1.6, R_2 = 14.2 \,\mathrm{kpc}$ ,  $\gamma = 2$ , and  $t = 3.3 \times 10^7 \,\mathrm{yr}$ . The solid lines represent the past status of the two galaxies and dotted lines do there future status.

The instability of the gaseous disks can be simply justified by the operating mechanism of the viscosity. When gas is piled up, the higher star formation rates can efficiently remove the angular momentum of gas, and then suppress the star formation rates. The system should be self-organized and stable. However, we should give a detail description of stability analysis in a future paper.

## 4. Applications

Dynamics of the gaseous disk presented here allows us to compare current model with Genzel et al.'s observations of star-forming galaxies at high-redshift. Observations of SIN-FONI on ESO VLT provide details of the "cold gas" accretion. We choose two galaxies as illustrations to apply the present theoretical model. BX 482 is a ring-dominated star-forming galaxy, of which the ring radius is  $R_{\rm ring} = 7.0 \pm 0.8 \rm kpc$  with a narrower width  $\Delta R \sim 1 \rm kpc$ , its dispersion velocity is  $\sigma = 210 \rm km~s^{-1}$  and the surface density of star formation rates is  $0.57 \pm 0.3 M_{\odot} \rm ~yr^{-1} \rm ~kpc^{-2}$ . We hence choose the ring model (eq. 8). The bright H $\alpha$  ring limits the lifetime of the ring, which is about  $\sim 10^7 \rm yr$  in light of OB stars. The left column of Figure 5 gives the dynamical evolution of the ring. The Toomre parameter Q shows that the ring is self-gravity dominated. A stellar ring formed in the gaseous ring is still growing shown by the red line, but the H $\alpha$  ring is becoming dimmer.

BzK 6004 is also a rotation-dominated galaxy with relatively faint but broader H $\alpha$  ring  $(\Delta R/R \sim 1.0 \text{ from Figure 5 in Genzel et al. 2008})$ . The ring radius is  $R_{\text{ring}} = 6.9 \pm 0.8 \text{kpc}$  and the dispersion velocity of galaxy is  $\sigma = 240 \text{km s}^{-1}$  and the surface density of star formation rate is  $0.6 \pm 0.3 M_{\odot} \text{ yr}^{-1} \text{ kpc}^{-2}$ . The current data does not allow us to distinguish the case of different  $\gamma$  we thus just use  $\gamma = 2$  as an illustration. The dynamical evolution of the galaxy is shown by the red line in the right column of Fig. 5. The current stage of the ring is approaching the end states of the star forming. The stellar ring is still growing fast and may remain as a wide stellar ring. The Q-value shows that self-gravity is also dominated.

We note that the solutions presented here tend to show an exponential stellar disk if the time is long enough. This agrees with the steady disks known for quite long time from Lin & Pringle (1987). The simple application of the current model shows here that SNexp does indeed play a key role in the dynamical evolution of the gaseous rings or disks. However, the application should be improved with the more detail data. For example, the good-quality data of  $H\alpha$  ring profile and the spatially resolved spectroscopy will allow us to get the evolution stage of gas and star formation from the stellar synthesis. Particularly, the very sharp inner edge of the ring predicted here is caused by SNexp. This reflects feedback of the star formation. Additionally, application of the present model to a large sample (e.g. Föster Schreiber et al. 2009) will produce the initial conditions of the sample for a statistics in future. This will be invaluable to justify the origin of the cold gas.

We would like to stress here that the present applications focus on the main features of galaxies at high-redshift. The ring or disk models for the two galaxies are less conclusive. We need more information of the galaxies, such as, stellar ages at different ring radii, so as to give more robust pictures. Degeneracies of parameters limit applications of the model.

#### 5. Conclusions

We set up a model of gaseous disk with star formation, in which the viscosity is driven by turbulence excited by SNexp. We get the analytical solutions for the initial condition of single gas ring, showing complicated secular evolutionary behaviors. Several different kinds of stellar distributions can be formed, including exponential types. The present model is able to reproduce starburst rings in two galaxies as illustrations.

The model will be improved in several aspects in future by using: (1) nonlinear star formation law, (2) separated equations of stars and gas, and (3) initially twisted gaseous disk (Lu & Cheng 1991). These will help us to get the initial conditions as a consequence of minor mergers and allow us to study the evolution of stellar disks and bulges.

The referee is greatly thanked for a very helpful report improving the manuscript. Prof. J.-F. Lu is acknowledged for useful discussions. We appreciate the stimulating discussions among the members of IHEP AGN group. The research is supported by NSFC-10733010 and 10821061, CAS-KJCX2-YW-T03, and 973 project (2009CB824800).

## REFERENCES

Bournaud, F., Jog, C. J. & Combes, F. 2007, A&A, 476, 1179

Bower, R. G. et al. 2006, MNRAS, 370,645

Brooks, A. M. et al. 2009, ApJ, 694, 396

Chen, Y.-M., Wang, J.-M., Yan, C.-S., Hu, C. & Zhang, S. 2009, ApJ, 695, L130

Daddi, E. et al. 2007, ApJ, 670,156

Davé, R. 2008, MNRAS, 385, 147

Dekel, A. et al. 2009, Nature, 457, 451

Dib, S., Bell, E. & Burkert A. 2006, ApJ, 638, 797

Dib, S. et al. 2009, arXiv:0903.2241

Dobbs, C. L. & Pringle, J. E. 2009, MNRAS, 396, 1579

Elbaz, D. et al. 2007, A&A, 468, 33

Föster Schreiber, N. M. et al. 2006, ApJ, 645,1062

Föster Schreiber, N. M. et al. 2009, ApJ, in press (arXiv:0903.1872)

Genzel, R. et al. 2006, Nature, 442, 786

Genzel, R. et al. 2008, ApJ, 687, 59

Guo, Q. & White, S. D. M. 2008, MNRAS, 384, 2

Hernquist, L. & Mihos, C. 1995, ApJ, 448, 41

Kato, S., Fukue, J. & Mineshige, S. 1998, Black-Hole Accretion Disks, Kyoto University Press, p571

Kawakatu, A. & Wada, K. 2008, ApJ, 681, 73

Kitzbichler, M. G. & White, S. D. M. 2007, MNRAS, 376, 2

Krumholz, M. R., McKee, C. F. & Tumlinson, J. 2009, ApJ, 693, 216

Law, D. R. et al. 2007, ApJ, 669, 929L

Lin, D. N. C. & Pringle, J. E. 1987, ApJ, 320, L87

Lu, J.-F. & Cheng, F.-H. 1991, Science China A (in Chinese), 9, 971

Lynden-Bell, D. & Pringle, J. E. 1974, MNRAS, 168, 603

Mac Low, M.-M. & Klessen, R. S. 2004, Rev. Mod. Phys., 76, 125

Naab, T. et al. 2007, ApJ, 658, 710

Noeske, K. G. et al. 2007, ApJ, 660, L43

Shakura, N. I. & Sunyaev, R. 1973, A&A, 24, 337

Tacconi, L. et al. 2006, ApJ, 640, 228

Tacconi, L. et al. 2008, ApJ, 680, 246

Thompson, T., Quataert, E. & Murray, N. 2005, ApJ, 630, 167

Vollmer, B. & Beckert, T. 2003, A&A, 404, 21

Wada, K. & Norman, C. 2002, ApJ, 566, L21

Wang, J.-M., Chen, Y.-M., Yan, C. S. & Hu, C. 2008, ApJ, 673, L9

Wang, J.-M., Hu, C., Li, Y.-R., Chen, Y.-M. et al.

Wang, J.-M., Chen, Y.-M. & Zhang, F. 2006, ApJ, 647, L17 2009, ApJ, 697, L14

Wright, S. A. 2007, ApJ, 658, 78

This preprint was prepared with the AAS IATEX macros v5.2.